



# Distinct Patterns of Automatic and Controlled Incongruent Information Processing in the Human Brain

Jialin Du<sup>1†</sup>, Yu Zhu<sup>1†</sup>, Chengtian Zhao<sup>1</sup>, Dongju Yang<sup>1</sup>, Tao Yu<sup>2</sup>, Xiaohua Zhang<sup>2</sup>, Liankun Ren<sup>1\*</sup> and Yuping Wang<sup>1,3,4\*</sup>

<sup>1</sup> Department of Neurology, Xuanwu Hospital, Capital Medical University, Beijing, China, <sup>2</sup> Department of Functional Neurosurgery, Beijing Institute of Functional Neurosurgery, Xuanwu Hospital, Capital Medical University, Beijing, China, <sup>3</sup> Institute of Sleep and Consciousness Disorders, Beijing Institute for Brain Disorders, Beijing, China, <sup>4</sup> Beijing Key Laboratory of Neuromodulation, Beijing, China

## OPEN ACCESS

### Edited by:

Jiaojian Wang,  
Kunming University of Science and  
Technology, China

### Reviewed by:

Chunlin Li,  
Capital Medical University, China  
Wei Shi,  
Beihang University, China

### \*Correspondence:

Yuping Wang  
doctorwangyuping@163.com  
Liankun Ren  
rlkbrain2000@yahoo.com

<sup>†</sup>These authors have contributed  
equally to this work

### Specialty section:

This article was submitted to  
Cognitive Neuroscience,  
a section of the journal  
Frontiers in Human Neuroscience

Received: 15 December 2021

Accepted: 29 March 2022

Published: 06 May 2022

### Citation:

Du J, Zhu Y, Zhao C, Yang D, Yu T,  
Zhang X, Ren L and Wang Y (2022)  
Distinct Patterns of Automatic and  
Controlled Incongruent Information  
Processing in the Human Brain.  
*Front. Hum. Neurosci.* 16:836374.  
doi: 10.3389/fnhum.2022.836374

It is a fundamental ability to discriminate incongruent information in daily activity. However, the underlying neural dynamics are still unclear. Using stereoelectroencephalography (SEEG), in this study, we investigated the fine-grained and different states of incongruent information processing in patients with refractory epilepsy who underwent intracranial electrode implantation. All patients performed a delayed match-to-sample paradigm in the sequential pairs of visual stimuli (S1 followed by S2). Participants were asked to discriminate whether the relevant feature of S2 was identical to S1 while ignoring the irrelevant feature. The spatiotemporal cortical responses evoked by different conditions were calculated and compared, respectively, in the context of brain intrinsic functional networks. In total, we obtained SEEG recordings from 241 contacts in gray matter. In the processing of irrelevant incongruent information, the activated brain areas included the superior parietal lobule, supramarginal gyrus, angular gyrus, inferior temporal gyrus, and fusiform gyrus. By comparing the relevant incongruent condition with the congruent condition, the activated brain areas included the middle frontal gyrus, superior temporal gyrus, middle temporal gyrus, posterior superior temporal sulcus, and posterior cingulate cortex. We demonstrated the dynamics of incongruent information processing with high spatiotemporal resolution and suggested that the process of automatic detection of irrelevant incongruent information requires the involvement of local regions and relatively few networks. Meanwhile, controlled discrimination of relevant incongruent information requires the participation of extensive regions and a wide range of nodes in the network. Furthermore, both the frontoparietal control network and default mode network were engaged in the incongruent information processing.

**Keywords:** incongruent information processing, stereoelectroencephalography, event-related potential, frontoparietal control network, default mode network

## INTRODUCTION

We detect, discriminate, and select incongruent information in daily life, representing the fundamental ability of cognitive control to guide thoughts and actions according to internal intentions (Breukelaar et al., 2017). It refers explicitly to ignoring goal-interfered information and emphasizing task-relevant stimulus information through the attentional biasing of perceptual

processing (Egner and Hirsch, 2005). Over the past few decades, efforts have been made to probe the dynamics of incongruent information processing. Accumulative evidence derived from neuroimaging and electrophysiological studies has shown that incongruent information processing involves activation and interactions among distributed cortical areas (Spreng et al., 2010; Cocchi et al., 2013; Cole et al., 2014). Compared with other methods, electroencephalography (EEG) offers an optimized approach due to the high time resolution.

At present, a range of evoked potentials in relation to incongruent information have been reported under various conditions using scalp EEG recordings. In the oddball or no-go/go task paradigms, the N2 component that was first described in the 1970s showing greater negative amplitude on incongruent trials than on congruent trials at ~200–350 ms after stimulus presentation was classically recognized. There is a general consensus that N2 is the essential functionally related cognitive control index (Larson et al., 2014; Xiao et al., 2020), which is likely to reflect incongruent monitoring (anterior N2) and interference processing (posterior N2) (Tian et al., 2014). Moreover, Kotchoubey and Kramer reported that a more significant negative potential with peak latencies of 200–300 ms was elicited in a memory search task when the memory set consisted of only single-item trials, in which the comparison and probe stimulus occurred in immediate succession (Kramer et al., 1991; Kotchoubey et al., 1996). Using sequential matching tasks in which participants were required to decide whether a second stimulus was the same or different from an initial stimulus, our prior series of studies consistently demonstrated that such a subcomponent of N2 was enhanced when the second stimulus in a pair did not match the first one (Wang et al., 1998, 2000). The findings were further confirmed by Kimura et al. in irrelevant stimulus dimensions, showing that the irrelevant-change trials elicited a more prominent frontocentral N270 component than no-change trials (Kimura et al., 2006).

The identification of the N2 subcomponent is speculated to reflect the intrinsic template-matching process. A better understanding of the question of how the brain processes incongruent information is essential to investigate the course of cognitive control. In particular, the accurate location of neural sources at different stages is still to be refined. Direct recording of neural activity, which is available in the clinical presurgical evaluation of refractory epilepsy, provides a unique opportunity to elucidate the spatiotemporal processing on fine temporal (subsecond) and spatial (subcentimeter) scales. Considering that the intrinsic brain circuitry function is essential to implement the cognitive task, in this study, we addressed the relevant incongruent information processing in the context of the functional networks by means of stereoelectroencephalography (SEEG) using a delayed match-to-sample paradigm.

## MATERIALS AND METHODS

### Participants and Implantation of SEEG Electrodes

In total, 10 right-handed patients (3 men and 7 women) with refractory epilepsy at Xuanwu Hospital Capital Medical

University who underwent presurgical evaluation with SEEG implantation were included. All patients had normal intelligence (IQ score above 80) and standard or corrected-to-normal vision. The SEEG implantation plan was determined based on clinical grounds. SEEG electrodes (HuaKe HengSheng, Beijing, China) were stereotactically implanted under general anesthesia. Each SEEG electrode consisted of a cylinder, 0.8 mm in diameter, and contained 10–16 contacts of 2 mm in length separated by 1.5 mm. The implanted number and placement of the electrodes were based solely on medical considerations. The procedure has been described in our previous study (Ren et al., 2020). After surgery, long-term monitoring was performed for ~7–14 days to capture the habitual epileptic seizures.

The research protocol was approved by the Institutional Review Board Committee of Xuanwu Hospital Capital Medical University, in accordance with the ethical standards of the Declaration of Helsinki. Patients were thoroughly informed about the purposes of the study and gave written informed consent.

### Reconstruction of SEEG Electrodes

To determine the precise location of the SEEG electrodes, postsurgery CT scans were linearly and subsequently non-linearly co-registered to the template T1-MRI image (MNI ICBM2009b NLIN, Asym) using Advanced Normalization Tools (ANTs, a toolbox that has been integrated into LEAD-DBS software, <http://www.lead-dbs.org>) (Horn et al., 2019). Then, the depth electrodes were readily detected three-dimensionally by visual inspection after normalization to template MNI, and contact locations were reconstructed using MATLAB (MathWorks Inc., Natick, MA, USA). This method has been validated in our previous study (Ren et al., 2020). All electrodes were automatically detected and classified according to parcellation of gray and white matter. Only contacts located in the gray matter were further analyzed.

Electrodes were categorized into the Yeo atlas 17-network (Yeo et al., 2011, 2014), according to the regions of interest as defined in the previous studies. In addition, the hippocampus was merged as the 18th cortical region.

### Experimental Procedure and SEEG Recording

After 3 days of electrode implantation surgery, the patient performed the task in a dimly lit, sound-attenuating room with response buttons under their hands. Visual stimuli were presented at the centre of the screen with a gray background. No seizures occurred in any of the patients during the preceding 12 h.

A delayed match-to-sample paradigm was used in this study, which has been validated in our previous study and by other research groups. The stimuli consisted of different shapes with different colors. The visual stimuli presented to each patient were controlled by a stimulus system (STIM2; Neurosoft Labs Inc., Sterling, VA, USA). Each trial consisted of a pair of sequentially presented stimuli: a first stimulus (S1), followed by a second stimulus (S2). S1 and S2 were presented on the screen for 500 ms each, with an interval of 200 ms. The interval between each pair of stimuli was 5 s. The stimulus pairs were classified into four conditions of equal presenting probability:

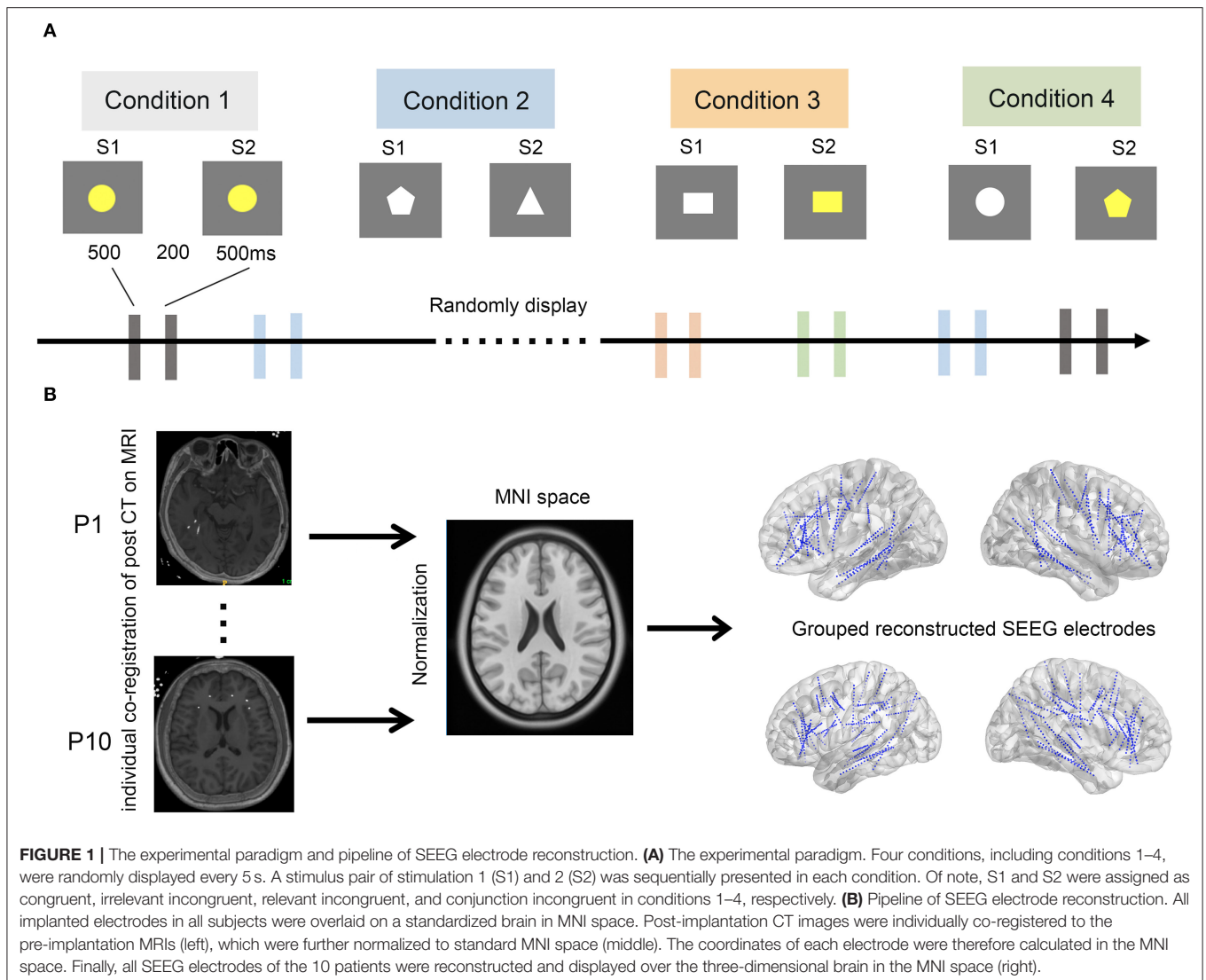


**FIGURE 1 |** The experimental paradigm and pipeline of SEEG electrode reconstruction. **(A)** The experimental paradigm. Four conditions, including conditions 1–4, were randomly displayed every 5 s. A stimulus pair of stimulation 1 (S1) and 2 (S2) was sequentially presented in each condition. Of note, S1 and S2 were assigned as congruent, irrelevant incongruent, relevant incongruent, and conjunction incongruent in conditions 1–4, respectively. **(B)** Pipeline of SEEG electrode reconstruction. All implanted electrodes in all subjects were overlaid on a standardized brain in MNI space. Post-implantation CT images were individually co-registered to the pre-implantation MRIs (left), which were further normalized to standard MNI space (middle). The coordinates of each electrode were therefore calculated in the MNI space. Finally, all SEEG electrodes of the 10 patients were reconstructed and displayed over the three-dimensional brain in the MNI space (right).

(i) S1 and S2 were identical (congruent condition); (ii) S2 was different from S1 in shape, same as S1 in color (irrelevant incongruent condition); (iii) S2 was different from S1 in color, same as S1 in shape (relevant incongruent condition); and (iv) different in both color and shape (conjunction incongruent condition) (**Figure 1**). The stimulus pairs of the four conditions were randomly presented in sequence. The whole task was divided into four blocks with a break of approximately 30 min in between to prevent fatigue in subjects. Patients were required to discriminate whether S1 and S2 were the same or not in color while ignoring their shapes and were instructed to press the corresponding keys on the keyboard as quickly and accurately as possible.

Stereoelectroencephalography data were recorded using the Neuroscan system (Scan 4.5; Neurosoft Labs Inc.) with a 128-channel SynAmps EEG/EP amplifier (Compumedics USA Inc., Charlotte, NC, USA) with a sampling rate of 2,000 Hz.

## Data Analysis of Local Field Potentials and Statistics

All SEEG data were processed using EEGLAB (<https://scn.ucsd.edu/eeqlab/>) and custom MATLAB codes unless stated otherwise.

Initially, the data were reviewed by visual inspection. The epoch that was contaminated with significant artifacts was discarded. Trials with incorrect responses and interictal epileptiform discharges were also excluded from further analysis. SEEG data were filtered with a bandpass of 0.5–150 Hz using a zero-phase shift finite impulse filter (Butterworth). After the notch filter at 50 Hz, epochs of all trials were extracted from 200 ms pre-S1 to 300 ms post-S2. Baseline correction was carried out using an interval of 200 ms (–200 ms pre-S1 to S1). The trials were automatically rejected when they contained neural activity that exceeded five standard deviations from the mean. More than 25 trials were averaged for each condition in each patient.

We next tested the significant differences between conditions. To address the spatial distribution of relevant incongruent processing, the responses on all the contacts were further classified according to the intrinsic functional networks. Using a two-sample *t*-test, two conditions, namely, congruent vs. irrelevant incongruent, congruent vs. relevant incongruent, and congruent vs. conjunction incongruent conditions of each contact within gray matter, were compared trail-by-trail in a time window of 0–800 ms from the point of S2 onset across each time point. Notably, the one-sample Kolmogorov–Smirnov test

was performed to confirm the distribution of the experimental data. To refine the relevant incongruent effect, correlations of congruent vs. irrelevant incongruent and congruent vs. conjunction incongruent conditions were evaluated, ranging from 200 to 300 ms after S2, respectively. A value of  $p < 0.05$  was considered to be statistically significant. To highlight spatiotemporal dynamics, a T map of relevant incongruent vs. congruent conditions was displayed (200–300 ms after S2 presentation).

Event-related potentials of each condition at all recorded sites were averaged and time-locked to S2 presentation. All data are presented as the mean  $\pm$  SEM.

**TABLE 1** | Basic information of the patients and the seizure onset zone.

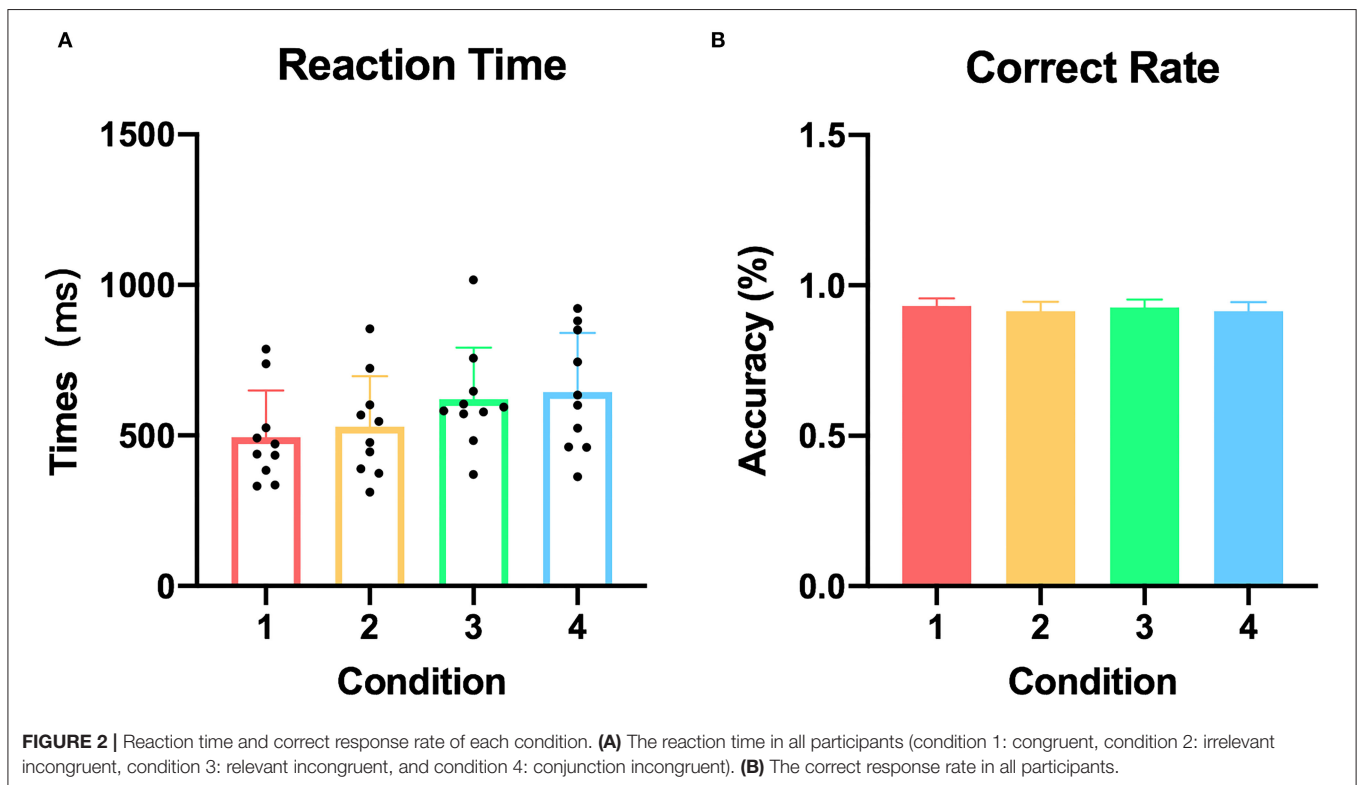
Patient number	Sex/Age	Hand laterality	Side of SEEG	Seizure onset zone
1	F/24	Right	Bilateral	Left superior frontal gyrus
2	M/23	Right	Left	Left temporal lobe
3	F/18	Right	Bilateral	Right temporal and hippocampus
4	M/21	Right	Bilateral	Right frontal lobe
5	F/18	Right	Right	Right frontal lobe
6	F/19	Right	Left	Left temporal lobe
7	F/28	Right	Left	Left temporal and hippocampus
8	M/18	Right	Right	Right inferior frontal gyrus
9	F/21	Right	Right	Right temporal lobe
10	F/23	Right	Left	Left frontal pole

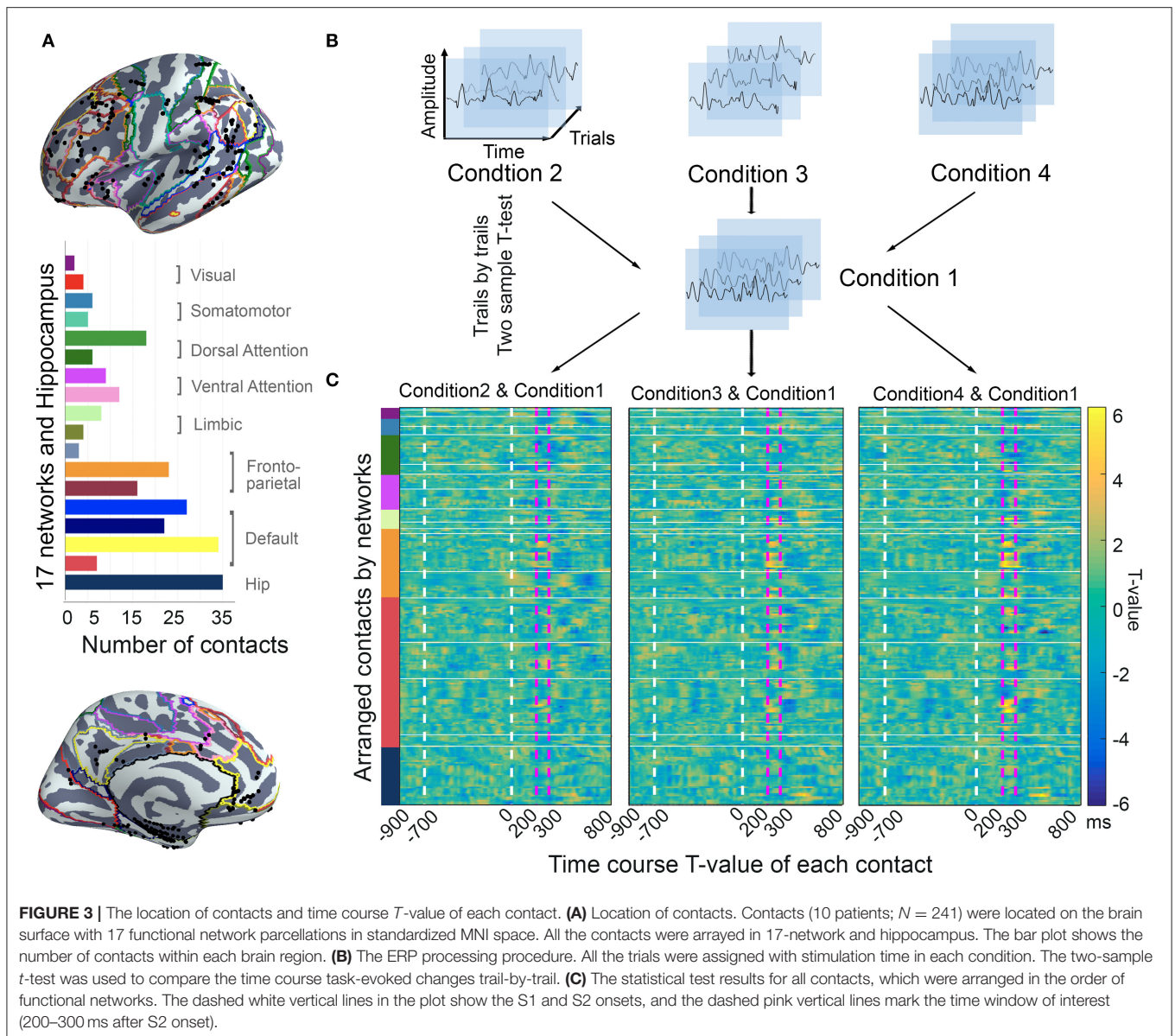
## RESULTS

### Subject Characteristics and Behavior

In total, 10 patients (3 men and 7 women) aged 18–28 years (with an average age of 21.3 years) were included in our study (Table 1). In total, we obtained SEEG recordings from 888 recording sites on 62 electrodes (Figure 1).

All participants performed the tasks successfully according to their behavioral performance with an average accuracy of 92.2%, and no difference was found among the four conditions ( $p = 0.952$ ). In addition, the mean reaction times did not differ between the congruent condition with the other three incongruent conditions, respectively ( $p_{\text{condition1\&condition2}} = 0.579$ ,  $p_{\text{condition1\&condition3}} = 0.063$ ,  $p_{\text{condition1\&condition4}} = 0.074$ ) (Figure 2).





## Time Courses of Task-Evoked Perturbation Distributed in Different Brain Intrinsic Networks

According to the anatomical atlas of gray and white matter, 241 contacts within gray matter were included for subsequent analysis. Guided by intrinsic network anatomy from functional neuroimaging in healthy populations, the electrodes were distributed throughout multiple cortical locations and were divided into a 17-network and hippocampus subsystems (Figure 3).

Using the two-sample  $t$ -test, we screened all 241 contacts for the voltage of task-evoked changes in the intrinsic networks during the time window of  $-900$  ms pre-S2 to  $800$  ms post-S2 presentation. Since our previous work showed that neural activity during 200–300 ms after S2 onset might be most relevant

to incongruent information processing, thus we focused further analysis on this time window. Obviously, the  $t$ -values of the contacts varied over the distributed anatomical locations, and they showed distinct effects among the functional networks by visual inspection.

To better evaluate the relationship between the relevant incongruent condition and congruent condition, coefficients were attained by correlating the mean  $t$ -value (200–300 ms) between the relevant incongruent condition and irrelevant incongruent condition ( $0.6095$ ,  $p < 0.001$ ), the relevant incongruent condition and conjunction incongruent condition ( $0.8325$ ,  $p < 0.001$ ), and the irrelevant incongruent condition and conjunction incongruent condition ( $0.6749$ ,  $p < 0.001$ ), respectively, suggesting the distinct responses to the relevant incongruent information (Figure 4).

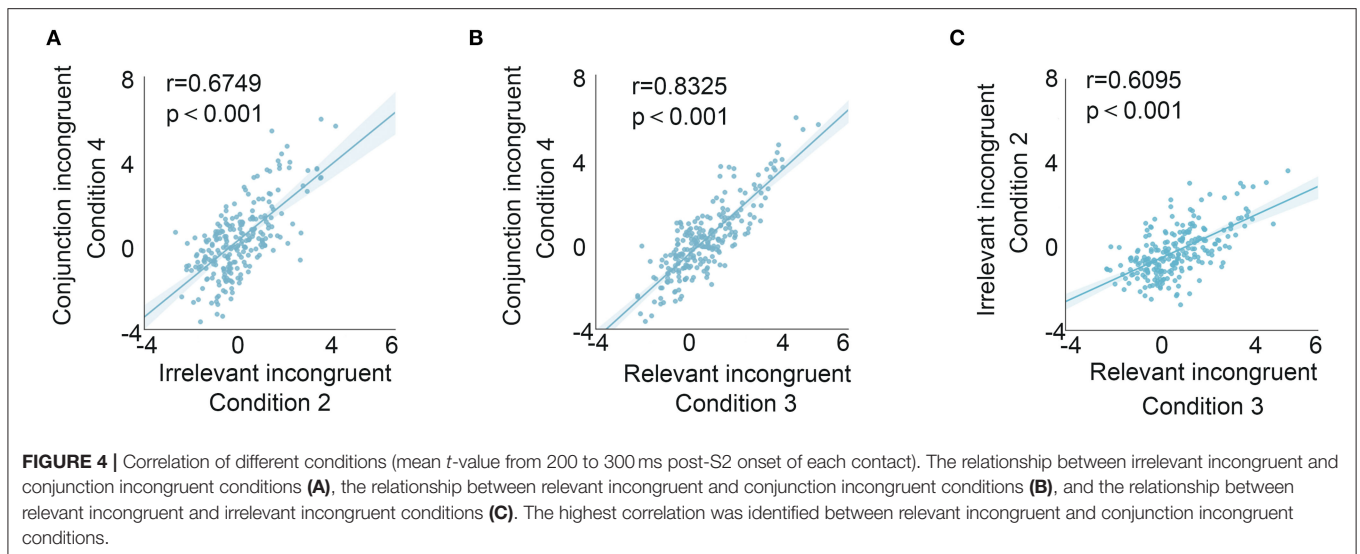


**TABLE 2** | The anatomical location of different brain areas involved in the different states of incongruent information processing.

Irrelevant incongruent & congruent	Relevant incongruent & congruent
Superior parietal gyrus	
Supramarginal gyrus	Supramarginal gyrus
Angular gyrus	Angular gyrus
	Middle frontal gyrus
	Superior temporal gyrus
	Middle temporal gyrus
Inferior temporal gyrus	
Fusiform gyrus	Fusiform gyrus
	Posterior superior temporal sulcus
	Posterior cingulate cortex

## Spatial Location of Different States in Incongruent Information Processing Irrelevant Incongruent Information Processing With Automatic Detection

To clarify the different states of incongruent information processing, we found the anatomical location of each contact with significant statistics in those comparisons, which suggested that the brain areas are involved in the different states in incongruent information processing (Table 2).

First, when detecting task-irrelevant incongruence, the subjects responded after S2 appeared even if they did not notice the relevant incongruence, speculating that this process may belong to automatic detection. We calculated the mean *t*-value after S2 onset between the irrelevant incongruent condition and the congruent condition. The core brain areas were concentrated in the superior parietal lobule, inferior parietal lobule (supramarginal gyrus, angular gyrus), inferior temporal gyrus, and fusiform gyrus.

Based on the anatomical boundaries defined by the literature, contacts were categorized into the 17-network and hippocampus subsystems. Focusing on the irrelevant incongruent condition,

the mean *t*-value compared with the congruent condition between 200 and 300 ms after S2 onset in all contacts indicated the specificity of spatial distribution in the parietal regions of the frontoparietal control network (FPCN) and temporal regions of the default mode network (DMN) (Figure 5).

## Relevant Incongruent Information Processing With Controlled Discrimination

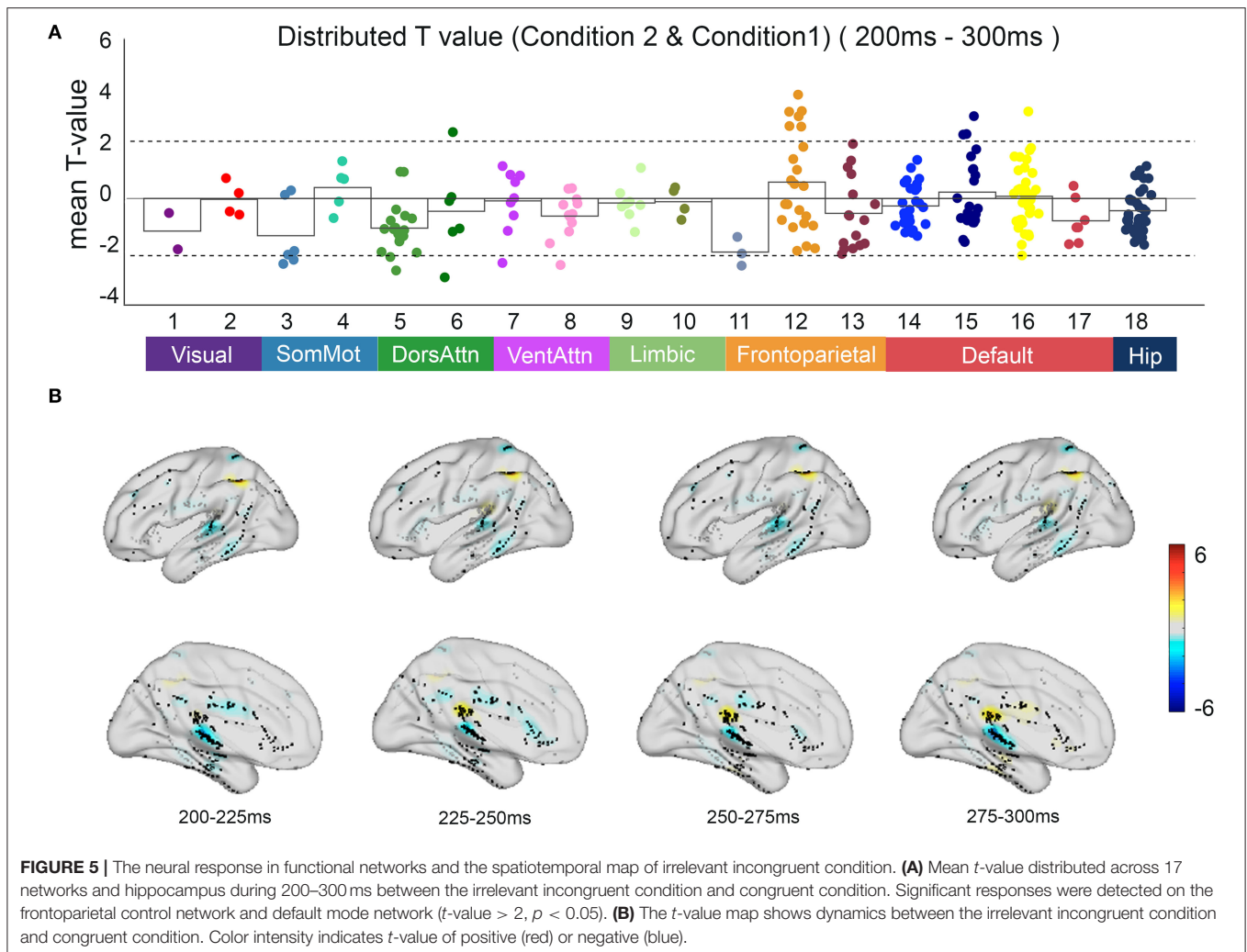
Furthermore, in the relevant incongruent condition, the subjects needed to identify whether the color feature was different between S1 and S2 in the relevant incongruent condition and the conjunction incongruent condition. The relevant incongruent information processing was referred to as controlled discrimination. We identified that the dynamics of task-evoked perturbation over a long period of time were more specific to incongruent information processing than to congruent information processing.

Compared with automatic detection, the brain regions that were activated for controlled discrimination included the frontal middle gyrus, superior temporal gyrus, middle temporal gyrus, posterior superior temporal sulcus, and posterior cingulate cortex. The T map showed the frontal regions of the FPCN and the PCC within the DMN engaged in the relevant incongruent information processing with statistical significance ( $p < 0.05$ ) (Figure 6).

To highlight the specific neural responses to relevant incongruent information, representative ERPs (condition 3 of relevant incongruent task minus condition 1 of congruent task) among different intrinsic functional networks were picked up for visual inspection. The results are displayed in Figure 7. Finally, schematic figures were conceived to characterize the dynamic profile of the human brain.

## DISCUSSION

Based on the direct recording of neural activity, our study reveals several vital points in incongruent information processing. First, we demonstrated the cortical dynamics with high temporal and

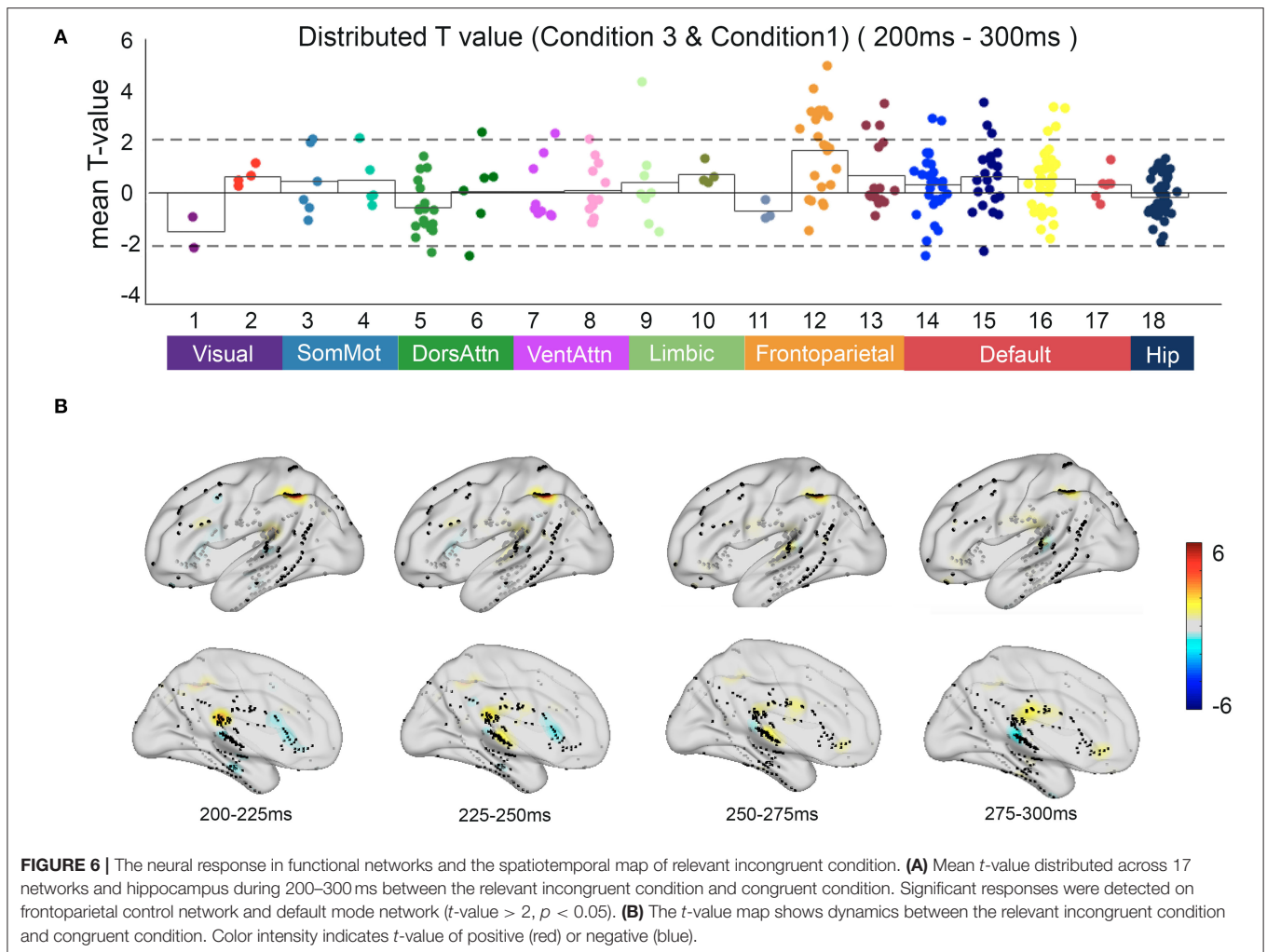


spatial resolutions during the delayed match-to-sample task. Our data indicated that the N2 subcomponents are responsible for the incongruent stimulus, consistent with previous findings (Bennett et al., 2014). Second, we identified the critical areas and networks involved in the processing of irrelevant and relevant incongruent information. Moreover, we suggested that there may be two integrated modalities of incongruent information processing in different states referred to as automatic detection and controlled discrimination.

A negative peak between 200 and 350 ms in scalp recording is defined as N2 since it follows a negative peak at  $\sim 100$  ms in the auditory modality or at around approximately 180 ms in the visual modality (Donkers and van Boxtel, 2004; Sur and Sinha, 2009). Hence, there has been an increased interest in the N2 components for understanding the nature and sequence of cognitive control that covers strategic monitoring and control of motor responses in recent years (Folstein and Van Petten, 2008). In fact, N2 comprises several subcomponents (N2a, N2b, and N2c) that can be elicited in different tasks under various conditions. More studies have focused on the N2a, which was

also termed auditory mismatch negativity (MMN) (Näätänen et al., 2007; Fishman, 2014), the N2b, which was consistently observed in oddball studies in the visual modality (Szucs et al., 2007), and the N2c, which was distinguished from the MMN and N2b and was modality-specific on scalp distribution, posteriorly in the visual modality but at the frontocentral area in the auditory modality. The scalp EEG results showed a large component that was sensitive to incongruent information and could be elicited during the interval of 200–300 ms after S2 presentation, i.e., in a pair of sequentially presented stimuli, the second stimulus was different from the first stimulus no matter what the attributes of the stimuli are, such as shapes, colors, numbers, and locations. Typically, participants judged whether two consecutively presented stimuli were congruent or incongruent in specific attributes in the delayed match-to-sample task (Szucs et al., 2007).

Such an incongruent-related N2 component was thought to reflect a process of stimulus discrimination, whereas the MMN complex and N2b complex were thought to index different stages of mismatch detection (Wu et al., 2010). In particular, N270,



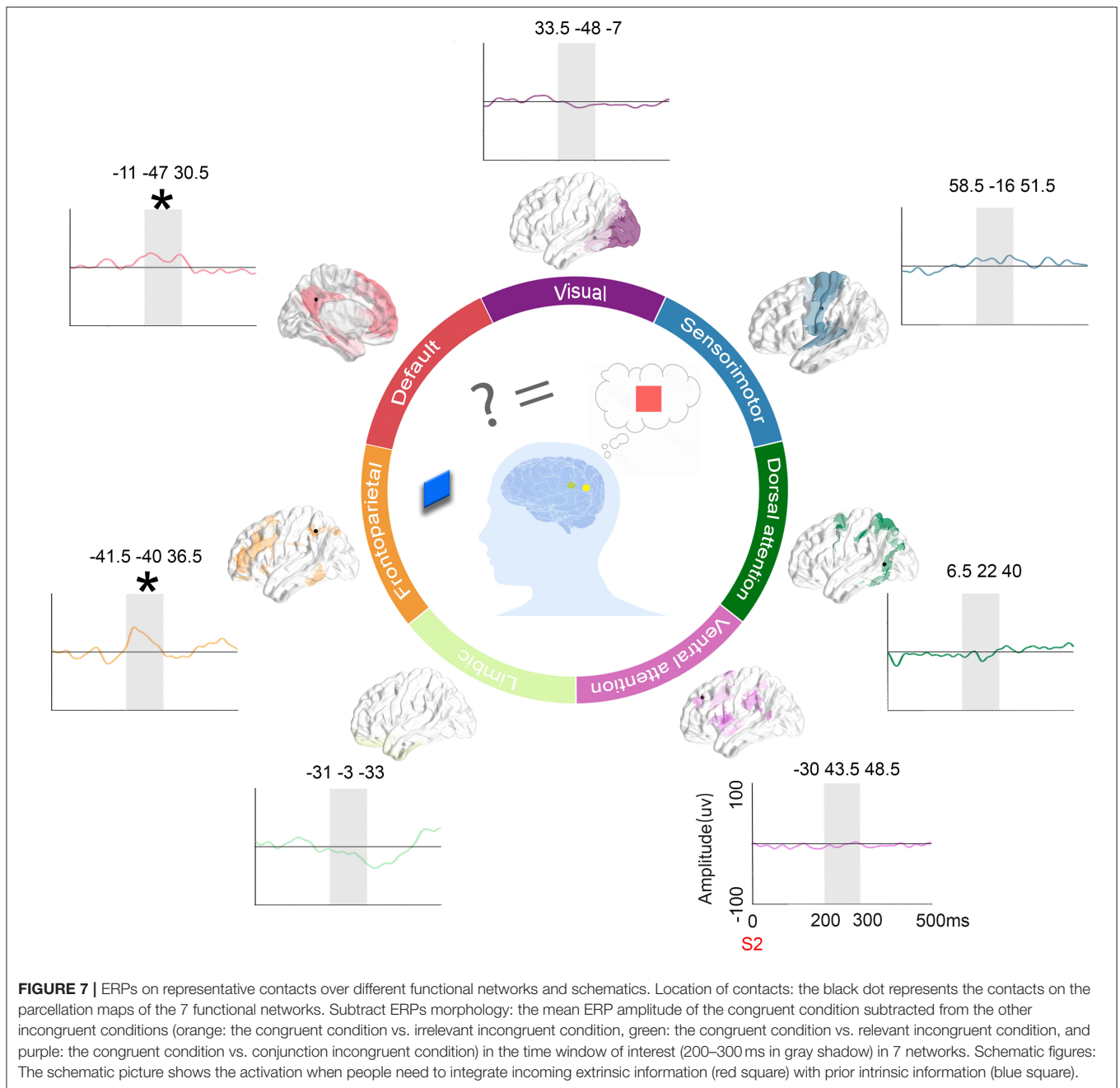
a negative ERP component with a peak latency of  $\sim 270$  ms, is speculated to reflect the processing of incongruent information and be influenced by attention. As a result, we indicated that the N2 subcomponents are responsible for the incongruent stimulus in the sequential matching paradigm, which was consistently confirmed by a series of studies (Wang et al., 1998, 2000, 2003; Cui et al., 2000; Bennett et al., 2014; Liang et al., 2017).

In this study, the application of SEEG offered the opportunity to probe the processing with high temporal and spatial resolutions. Technically, the bipolar montage of consecutive adjacent contacts is traditionally employed to attenuate the volume effects. Nevertheless, the polar of N2 recorded intracranially was different from that of scalp EEG. Hence, we compared the evoked potentials with baseline activity and tested for significance by utilizing a two-sample  $t$ -test for every data point between the two conditions, which was data-driven and did not make any assumptions about when the effect was expected (Guthrie and Buchwald, 1991; Piai et al., 2015). The significance between conditions was speculated to avoid the polar issue.

Our data showed the specific responses to both irrelevant and relevant incongruent tasks. Prominent statistical significance was

detected in the incongruent task specifically compared with the congruent task between 200 and 300 ms after the S2 presentation. Importantly, our research suggests that different brain regions are responsible for different states of incongruent information.

In the irrelevant incongruent condition, although we ignored the feature of shape, there were also significant changes when compared with the congruent condition. Our results demonstrated that some essential areas, the superior parietal lobule, inferior parietal lobule (supramarginal gyrus and angular gyrus), inferior temporal gyrus, and fusiform gyrus, were significantly activated during this processing. Studies from primates have shown that parietal neurons are activated earlier during bottom-up attention (Buschman and Miller, 2007). Evidence from neuroimaging studies suggests that the inferior parietal lobule participates in the bottom-up perception that is uniquely human (Igelstrom and Graziano, 2017). Notably, a similar SEEG study revealed the contribution of the rostral inferior parietal lobule in decision processing (Ter Wal et al., 2020). Particularly, more recent studies revealed that human parietal areas played a central role in feature detection decisions (Guidotti et al., 2019), which is assumed to be integrated



into incongruent condition control processing. The inferior temporal gyrus, as part of the visual ventral pathway, is associated with object, face, and scene perception, and studies of single-cell electrophysiological recordings from primates directly confirm the involvement of the inferior temporal gyrus in object recognition (Gross, 2008; Conway, 2018). From the view of functional networks, the inferior parietal lobule is a part of the FPCN, which is considered to support cognitive control and decision-making processes (Martin-Signes et al., 2019). Meanwhile, the temporal regions of the DMN were also involved in the processing of irrelevant incongruent information,

which indicated that the detection of irrelevant incongruent information may be automatic.

Moreover, by comparing the relevant incongruent condition with the congruent condition, we speculated that the activated brain regions were involved in the feature-controlled discrimination processing, including the inferior parietal lobule (supramarginal gyrus and angular gyrus), middle frontal gyrus, superior temporal gyrus, middle temporal gyrus, fusiform gyrus, posterior superior temporal sulcus, and posterior cingulate cortex. The frontal regions, such as the middle frontal gyrus, are part of the FPCN, which plays a key role in the top-down

control of attention. Additionally, the middle frontal gyrus is considered to be the convergence point of the dorsal and ventral attention networks. In addition, the superior temporal gyrus, middle temporal gyrus, fusiform gyrus, and posterior superior temporal sulcus participated in the relevant incongruence feature discrimination. Interestingly, we detected the involvement of the PCC in goal-driven incongruent information attention, which has not yet been described. The PCC is one of the cores of the DMN, which may be related to the problem-solving and executive control processes (Andrews-Hanna et al., 2010; Leech and Sharp, 2014). In addition to the classical concept that DMN increases its activity during passive states and decreases its activity during positive states, recent studies reported the DMN as an active and dynamic “sense-making” network that integrates incoming extrinsic information with prior intrinsic information (Yeshurun et al., 2021). In our paradigm, the S1 stimulus represents the intrinsic information, and the S2 stimulus represents the incoming information. The results suggested that different brain regions are significantly activated when processing target-relevant incongruent information, which indicated that the discrimination processing of relevant incongruent information may require controlled attention.

There are also some limitations in our research. First, the potential impact of an altered brain network should be noted because the participants were patients with presurgical epilepsy. To minimize the confounding effects of epilepsy on the acquired intracranial electrophysiological data, rigorous methods were adopted in this study: only patients with focal epilepsies who have normal intelligence were studied; only patients with a few localized deficits were included; all obtained data were several hours outside the window of seizures; and only the channels that are free of pathological activity were included at the individualized level (Parvizi and Kastner, 2018). Second, the number of patients was limited. Accordingly, the brain regions were not covered completely. For example, SEEG electrodes were sparsely implanted in the dorsal lateral prefrontal cortex and dorsal anterior cingulate in our patient group since the placement of the electrodes was determined by clinical ground only.

In summary, this study showed the fine-grained dynamics of incongruent information processing, and our results offer new insights into the refined understanding of how the brain processes incongruent information. We suggested that there may be two integrated modalities of incongruent information processing in different states referred to as automatic detection and controlled discrimination. The process of automatic detection of disparity information requires the involvement of a few brain regions with networks, such as the parietal regions of the FPCN and inferior temporal gyrus of the DMN. Furthermore, controlled discrimination of incongruence information requires the involvement of wider networks and a wide range of nodes in the network, including the frontal lobe of the FPCN and the PCC of the DMN. There may be a spatiotemporal interaction between the networks in incongruent information processing. The integrated brain network collaboration model may be an important modal of the cognitive control process that deserves more research in the future.

## DATA AVAILABILITY STATEMENT

The raw data supporting the conclusions of this article will be made available by the authors, without undue reservation.

## ETHICS STATEMENT

The studies involving human participants were reviewed and approved by Xuanwu Hospital, Capital Medical University. The patients/participants provided their written informed consent to participate in this study.

## SIGNIFICANCE STATEMENT

It is the fundamental ability to discriminate incongruent information through the attentional biasing of perceptual processing. Scalp electroencephalography and neuroimaging offer an optimized approach to probe the time course of incongruent information processing. However, the knowledge of such neural dynamics has not yet been defined. Therefore, it is necessary to refine how the brain processes incongruent information. We used SEEG recordings from patients with intractable focal epilepsy during the delayed match-to-sample task and demonstrated the cortical dynamics with high temporal and spatial resolutions. Moreover, we identified the critical cortical areas processing the incongruent information over the frontoparietal control network and default mode network. Our results will offer new insights into the refined understanding of how the brain processes incongruent information.

## AUTHOR CONTRIBUTIONS

JD: formal analysis and writing—original draft. YZ and DY: investigation and editing. LR: methodology and writing—review and editing. TY and XZ: resources. LR and YW: conceptualization and supervision. All authors contributed to the article and approved the submitted version.

## FUNDING

This work was supported by grants from the National Natural Science Foundation of China (Nos. 81771398 and 82071454) and the Beijing Natural Science Foundation (No. 7202062). This work is also supported by National Science and Technology Resources Sharing Service Platform Program (2016YFC1000307).

## ACKNOWLEDGMENTS

We would like to thank Yunzhe Liu, Ph.D. and Dr. Na Clara Pan for their critical discussions. We thank the patients for their cooperation in this study.

## REFERENCES

- Andrews-Hanna, J. R., Reidler, J. S., Sepulcre, J., Poulin, R., and Buckner, R. L. (2010). Functional-anatomic fractionation of the brain's default network. *Neuron* 65, 550–562. doi: 10.1016/j.neuron.2010.02.005
- Bennett, M. A., Duke, P. A., and Fuggetta, G. (2014). Event-related potential N270 delayed and enhanced by the conjunction of relevant and irrelevant perceptual mismatch. *Psychophysiology* 51, 456–463. doi: 10.1111/psyp.12192
- Breukelaar, I. A., Antees, C., Grieve, S. M., Foster, S. L., Gomes, L., Williams, L. M., et al. (2017). Cognitive control network anatomy correlates with neurocognitive behavior: a longitudinal study. *Hum. Brain Mapp.* 38, 631–643. doi: 10.1002/hbm.23401
- Buschman, T. J., and Miller, E. K. (2007). Top-down versus bottom-up control of attention in the prefrontal and posterior parietal cortices. *Science* 315, 1860–1862. doi: 10.1126/science.1138071
- Cocchi, L., Zalesky, A., Fornito, A., and Mattingley, J. B. (2013). Dynamic cooperation and competition between brain systems during cognitive control. *Trends Cogn. Sci.* 17, 493–501. doi: 10.1016/j.tics.2013.08.006
- Cole, M. W., Repovs, G., and Anticevic, A. (2014). The frontoparietal control system: a central role in mental health. *Neuroscientist* 20, 652–664. doi: 10.1177/1073858414525995
- Conway, B. R. (2018). The organization and operation of inferior temporal cortex. *Annu. Rev. Vis. Sci.* 4, 381–402. doi: 10.1146/annurev-vision-091517-034202
- Cui, L., Wang, Y., Wang, H., Tian, S., and Kong, J. (2000). Human brain sub-systems for discrimination of visual shapes. *Neuroreport* 11, 2415–2418. doi: 10.1097/00001756-20000830-00015
- Donkers, F. C., and van Boxtel, G. J. (2004). The N2 in go/no-go tasks reflects conflict monitoring not response inhibition. *Brain Cogn.* 56, 165–176. doi: 10.1016/j.bandc.2004.04.005
- Egner, T., and Hirsch, J. (2005). The neural correlates and functional integration of cognitive control in a Stroop task. *Neuroimage* 24, 539–547. doi: 10.1016/j.neuroimage.2004.09.007
- Fishman, Y. I. (2014). The mechanisms and meaning of the mismatch negativity. *Brain Topogr.* 27, 500–526. doi: 10.1007/s10548-013-0337-3
- Folstein, J. R., and Van Petten, C. (2008). Influence of cognitive control and mismatch on the N2 component of the ERP: a review. *Psychophysiology* 45, 152–170. doi: 10.1111/j.1469-8986.2007.00602.x
- Gross, C. G. (2008). Single neuron studies of inferior temporal cortex. *Neuropsychologia* 46, 841–852. doi: 10.1016/j.neuropsychologia.2007.11.009
- Guidotti, R., Tosoni, A., Perrucci, M. G., and Sestieri, C. (2019). Choice-predictive activity in parietal cortex during source memory decisions. *Neuroimage* 189, 589–600. doi: 10.1016/j.neuroimage.2019.01.071
- Guthrie, D., and Buchwald, J. S. (1991). Significance testing of difference potentials. *Psychophysiology* 28, 240–244. doi: 10.1111/j.1469-8986.1991.tb00417.x
- Horn, A., Li, N., Dembek, T. A., Kappel, A., Boulay, C., Ewert, S., et al. (2019). Lead-DBS v2: Towards a comprehensive pipeline for deep brain stimulation imaging. *Neuroimage* 184, 293–316. doi: 10.1016/j.neuroimage.2018.08.068
- Igelstrom, K. M., and Graziano, M. S. A. (2017). The inferior parietal lobule and temporoparietal junction: a network perspective. *Neuropsychologia* 105, 70–83. doi: 10.1016/j.neuropsychologia.2017.01.001
- Kimura, M., Katayama, J., and Murohashi, H. (2006). An ERP study of visual change detection: effects of magnitude of spatial frequency changes on the change-related posterior positivity. *Int. J. Psychophysiol.* 62, 14–23. doi: 10.1016/j.ijpsycho.2005.11.005
- Kotchoubey, B. I., Jordan, J. S., Grozinger, B., Westphal, K. P., and Kornhuber, H. H. (1996). Event-related brain potentials in a varied-set memory search task: a reconsideration. *Psychophysiology* 33, 530–540. doi: 10.1111/j.1469-8986.1996.tb02429.x
- Kramer, A. F., Strayer, D. L., and Buckley, J. (1991). Task versus component consistency in the development of automatic processing: a psychophysiological assessment. *Psychophysiology* 28, 425–437. doi: 10.1111/j.1469-8986.1991.tb00726.x
- Larson, M. J., Clayson, P. E., and Clawson, A. (2014). Making sense of all the conflict: a theoretical review and critique of conflict-related ERPs. *Int. J. Psychophysiol.* 93, 283–297. doi: 10.1016/j.ijpsycho.2014.06.007
- Leech, R., and Sharp, D. J. (2014). The role of the posterior cingulate cortex in cognition and disease. *Brain* 137, 12–32. doi: 10.1093/brain/awt162
- Liang, T., Hu, Z., Li, Y., Ye, C., and Liu, Q. (2017). Electrophysiological correlates of change detection during delayed matching task: a comparison of different references. *Front. Neurosci.* 11:527. doi: 10.3389/fnins.2017.00527
- Martin-Signes, M., Paz-Alonso, P. M., and Chica, A. B. (2019). Connectivity of frontoparietal regions reveals executive attention and consciousness interactions. *Cereb. Cortex* 29, 4539–4550. doi: 10.1093/cercor/bhy332
- Naatanen, R., Paavilainen, P., Rinne, T., and Alho, K. (2007). The mismatch negativity (MMN) in basic research of central auditory processing: a review. *Clin. Neurophysiol.* 118, 2544–2590. doi: 10.1016/j.clinph.2007.04.026
- Parvizi, J., and Kastner, S. (2018). Promises and limitations of human intracranial electroencephalography. *Nat. Neurosci.* 21, 474–483. doi: 10.1038/s41593-018-0108-2
- Piai, V., Dahslatt, K., and Maris, E. (2015). Statistically comparing EEG/MEG waveforms through successive significant univariate tests: how bad can it be? *Psychophysiology* 52, 440–443. doi: 10.1111/psyp.12335
- Ren, L., Yu, T., Wang, D., Wang, X., Ni, D., Zhang, G., et al. (2020). Subthalamic nucleus stimulation modulates motor epileptic activity in humans. *Ann. Neurol.* 88, 283–296. doi: 10.1002/ana.25776
- Spreng, R. N., Stevens, W. D., Chamberlain, J. P., Gilmore, A. W., and Schacter, D. L. (2010). Default network activity, coupled with the frontoparietal control network, supports goal-directed cognition. *Neuroimage* 53, 303–317. doi: 10.1016/j.neuroimage.2010.06.016
- Sur, S., and Sinha, V. K. (2009). Event-related potential: an overview. *Ind. Psychiatry J.* 18, 70–73. doi: 10.4103/0972-6748.57865
- Szucs, D., Soltesz, F., Czizler, I., and Csepe, V. (2007). Electroencephalography effects to semantic and non-semantic mismatch in properties of visually presented single-characters: the N2b and the N400. *Neurosci. Lett.* 412, 18–23. doi: 10.1016/j.neulet.2006.08.090
- Ter Wal, M., Platonov, A., Cardellachio, P., Pelliccia, V., LoRusso, G., Sartori, I., et al. (2020). Human stereoEEG recordings reveal network dynamics of decision-making in a rule-switching task. *Nat. Commun.* 11:3075. doi: 10.1038/s41467-020-16854-w
- Tian, Y., Liang, S., and Yao, D. (2014). Attentional orienting and response inhibition: insights from spatial-temporal neuroimaging. *Neurosci. Bull.* 30, 141–152. doi: 10.1007/s12264-013-1372-5
- Wang, Y., Kong, J., Tang, X., Zhuang, D., and Li, S. (2000). Event-related potential N270 is elicited by mental conflict processing in human brain. *Neurosci. Lett.* 293, 17–20. doi: 10.1016/S0304-3940(00)01480-4
- Wang, Y., Tang, X., Kong, J., Zhuang, D., and Li, S. (1998). Different systems in human brain are involved in presemantic discrimination of pictures as revealed by event-related potentials. *Neurosci. Lett.* 257, 143–146. doi: 10.1016/S0304-3940(98)00828-3
- Wang, Y., Tian, S., Wang, H., Cui, L., Zhang, Y., and Zhang, X. (2003). Event-related potentials evoked by multi-feature conflict under different attentive conditions. *Exp. Brain Res.* 148, 451–457. doi: 10.1007/s00221-002-1319-y
- Wu, J., Mai, X., Yu, Z., Qin, S., and Luo, Y. J. (2010). Effects of discrepancy between imagined and perceived sounds on the N2 component of the event-related potential. *Psychophysiology* 47, 289–298. doi: 10.1111/j.1469-8986.2009.00936.x
- Xiao, F., Sun, T., Cai, X. L., and Chen, Q. F. (2020). Task relevance effect on number/shape conflict detection in the number-matching task: an ERP study. *Acta Psychol.* 208:103126. doi: 10.1016/j.actpsy.2020.103126
- Yeo, B. T., Krienen, F. M., Chee, M. W., and Buckner, R. L. (2014). Estimates of segregation and overlap of functional connectivity networks in the human cerebral cortex. *Neuroimage* 88, 212–227. doi: 10.1016/j.neuroimage.2013.10.046
- Yeo, B. T., Krienen, F. M., Sepulcre, J., Sabuncu, M. R., Lashkari, D., Hollinshead, M., et al. (2011). The organization of the human cerebral cortex estimated by intrinsic functional connectivity. *J. Neurophysiol.* 106, 1125–1165. doi: 10.1152/jn.00338.2011
- Yeshurun, Y., Nguyen, M., and Hasson, U. (2021). The default mode network: where the idiosyncratic self meets the shared social

world. *Nat. Rev. Neurosci.* 22, 181–192. doi: 10.1038/s41583-020-00420-w

**Conflict of Interest:** The authors declare that the research was conducted in the absence of any commercial or financial relationships that could be construed as a potential conflict of interest.

**Publisher's Note:** All claims expressed in this article are solely those of the authors and do not necessarily represent those of their affiliated organizations, or those of the publisher, the editors and the reviewers. Any product that may be evaluated in

this article, or claim that may be made by its manufacturer, is not guaranteed or endorsed by the publisher.

*Copyright © 2022 Du, Zhu, Zhao, Yang, Yu, Zhang, Ren and Wang. This is an open-access article distributed under the terms of the Creative Commons Attribution License (CC BY). The use, distribution or reproduction in other forums is permitted, provided the original author(s) and the copyright owner(s) are credited and that the original publication in this journal is cited, in accordance with accepted academic practice. No use, distribution or reproduction is permitted which does not comply with these terms.*